P. BAZARNIK*,   M. LEWANDOWSKA*,   K.J. KURZYDŁOWSKI*

MECHANICAL BEHAVIOUR OF ULTRAFINE GRAINED Al-Mg ALLOYS OBTAINED BY DIFFERENT PROCESSING ROUTES

WŁAŚCIWOŚCI MECHANICZNE ULTRA DROBNOZIARNISTYCH STOPÓW Al-Mg OTRZYMANYCH RÓŻNYMI METODAMI

The subject of the study were microstructure and mechanical properties of two commercial 5xxx aluminium alloys obtained by Plastic Consolidation (PC) of nanopowders and Hydrostatic extrusion (HE). It has been observed that HE samples exhibit a higher strength whereas PC samples higher ductility. The two types of samples also differ in the type and intensity of serrations on stress-strain curves. The microstructures of samples processed were found to differ significantly in terms of size and shape of grains, grain boundary characteristics, second phase particles content and density of dislocations. The results are discussed in terms of the influence of microstructure on mechanical behaviour of 5xxx aluminium alloys processed by severe plastic deformation.

Keywords: Transmission Electron Microscopy, Portevin-Le Chatelier effect, Strengthening mechanisms, Ultrafine grained

W poniższej pracy badano właściwości mechaniczne dwóch komercyjnych ultra drobnoziarnistych stopów aluminium serii 5xxx otrzymanych przez Konsolidację Plastyczną (PC) nanoproszków oraz przez Wyciskanie Hydrostatyczne (HE). Mikrostruktury badanych próbek znacząco się różniły, w szczególności pod względem wielkości ziarna i charakteru granic ziaren. Badania właściwości mechanicznych pokazały, że obie próbki wykazują znakomite właściwości wytrzymałościowe (w obu próbkach granica plastyczności przekracza 450 MPa), jednakże próbki HE wykazują wyższą wytrzymałość, podczas gdy próbki PC większą plastyczność. Wyniki przedstawiono w formie analizy wpływu mikrostruktury na właściwości mechaniczne stopów aluminium serii 5xxx otrzymanych technikami dużego odkształcenia plastycznego. Wysokie właściwości mechaniczne przypisano różnorodnym mechanizmom umacniającym i funkcjonującym w tych próbkach, włączając w to: umocnienie roztworowe, umocnienie wydzieleniowe oraz umocnienie granicami ziaren i dyslokacyjne. Uzyskane wyniki wskazują na to, że mikrostruktura ma znaczący wpływ nie tylko na właściwości mechaniczne, ale również na typ ząbkowania na krzywych rozciągania.

1. Introduction

Commercial coarse-grained Al-Mg (5xxx series) alloys are broadly applied in demanding structural applications due to their economic price, low density, good strength, corrosion resistance and high formability [1,2,3]. Since precipitation strengthening is inefficient in the case of Al-Mg alloys [4], the enhancement in their mechanical properties can be achieved either by work hardening or grain size refinement below $1\mu m$. The latter is quantitatively described by the well-known Hall-Petch relationship [5].

Ultrafine grained (UFG) metals with the grain size in the submicrometer (100 nm – $1\mu m$) range can be obtained in a number of ways, which in general can be grouped into top-down and bottom-up methods. The top-down techniques usually involve Severe Plastic Deformation, e.g. Equal Channel Angular Pressing [6,7], High Pressure Torsion [6,8], Cyclic Extrusion Compression [6,9] and Multi Axial Forging [10], Cryo-milling and Cryo-rolling [11,12] and Hydrostatic Extrusion (HE) [13,14]. During the SPD processing, micrograined structures refine UFG via generation and rearrangement of defects, primarily dislocations. In a bottom-up approach, UFG structure of bulk materials is obtained via synthesis of powder precursors as the first step, followed by their consolidation at evaluated temperatures [15].

UFG structures obtained by top-down and bottom-up approaches differ substantially in terms of grain size, dislocation density, grain boundaries characteristics, the distribution of chemical components, and grain shapes, which in turn impart their spe-

* WARSAW UNIVERSITY OF TECHNOLOGY, FACULTY OF MATERIALS SCIENCE AND ENGINEERING, 02-507 WARSZAWA, 141 WOLOSKA STR., POLAND

cific mechanical properties [16]. The goal of this work was to develop UFG Al-5Mg-1Mn alloys using original SPD based processing paths, namely top-down SPD nano-refinement by HE and bottom-up nano-consolidation of nano-powders.

2. Experimental

The materials used in the present study were commercial Al-5Mg-1Mn (5XXX series) aluminium alloys. Nano-refinement was accomplished by HE of 5483 alloy billet at room temperature. The processing was conducted in three consecutive passes from initial diameter of 20 mm to 10 mm, 5 mm and 3 mm, respectively. The total true strain was 3.8. HE experiments were carried out at the Institute of High Pressure Physics of the Polish Academy of Sciences. Samples produced by plastic consolidation (PC) were obtained from rapidly solidified (cooling rate exceeding 10,000 K/s) flakes of 5083 alloy obtained via melt spinning process (RSP Technology). The flakes were consolidated via extrusion at a temperature of 420°C with an extrusion ratio of 25. Plastic consolidation was carried out in a protective atmosphere. The samples were in the form of 5 mm rods. The chemical compositions of alloys (5483, 5083) used in the present study are given in Table 1.

Detailed description of the microstructures of the HE and PC samples was performed by TEM observations of thin foils cut perpendicularly to the extrusion direction. Two microscopes were used to this end: TEM JEOL 1200EX at the accelerating voltage of 120kV and HITACHI HD-2700 at the accelerating voltage of 200kV. The analyses included: grains size and shape measurements, dislocation density measurements, precipitates identification and grain boundaries analysis in terms of the distribution of grain boundary misorientation angles.

The grain size was described using the equivalent grain diameter d which is defined as the diameter of a circle of the area equal to the surface area of a given grain. Average grain size and grain size distributions were determined by measuring more than 1000 grains for each alloy sample. The misorientation angles of individual grain boundaries were calculated from Kikuchi Line Diffraction Patterns. These patterns were subsequently used to calculate crystallographic orientation of individual grains and misorientation across grain boundaries by using KILIN and DES software developed at AGH University of Technology. HR STEM (High Resolution Scanning Transmission Electron Microscopy) observations and EELS (Electron Energy Loss Spectrometry) analyses were used in order to identify chemical compositions of precipitates and possible oxide segregation at the grain level.

Dislocation densities were estimated from TEM images using the equation:

$$\rho = \frac{N}{L_r t} \qquad (1)$$

where N is a number of dislocations which were cut by the projected lines, Lr is the total line length of random lines, and t is foil thickness [17]. Because of small grain size in both samples, not all grains in TEM imaging follow the Bragg law, which means that not all dislocations were visible, even if the sample was observed at different twist angles. The second important factor is TEM foils thickness (measured by EELS analysis), which varied between 50-150 nm. Because of these two factors, the error of this method was set at 10%.

In order to characterise mechanical properties, the samples cut from rods were subjected to tensile tests. The strain rate was about 10^{-4} s^{-1}. All tensile tests were carried out at the Dynamic testing machine MTS 858 Table Top System. Strain was measured by an extensometer with a base of 15mm.

In order to reveal the operating mechanisms of plastic deformation microscopic observations were carried out of the samples subjected to the tensile tests. TEM samples were cut from a depth of 1 mm below the fracture surfaces. The fracture surfaces were also examined with a scanning electron microscope Hitachi SU-70. Also measured were microhardness profiles near to them.

TABLE 1

Chemical composition of AA 5083 and 5483

Chemical composition [wt %]	Si	Fe	Cu	Mn	Mg	Cr	Zn	Ti	Others
5083 (PC)	max 0,30	max 0,40	max 0,10	0,4 – 1,0	4,0 – 4,9	max 0,25	max 0,25	max 0,10	max 0,05
5483 (HE)	max 0,20	max 0,15	max 0,05	0,55 – 1,0	4,5 – 5,0	max 0,20	max 0,20	max 0,05	Zr max 0,20

3. Results

3.1. Microstructure

TEM analysis revealed ultra-fine grained structures in both HE and PC samples (Fig. 1). However, these microstructures significantly differ in terms of the grain size and dislocation density. The microstructure of PC samples consists of grains of ˜460 nm with a relatively low dislocation density of $1 - 2 \cdot 10^{13}$ m^{-2}. In HE samples, the average grain size is much smaller ˜210 nm and grains are regular in shape with only a small tendency to elongation. A characteristic feature of this microstructure is the high density of dislocations estimated at 10^{16} m^{-2}

uniformly distributed inside the grains. The grain size distributions in both samples (Fig. 2) are log-normal. However, the HE samples feature much wider distribution indicating a lower homogeneity of the grain size.

TEM analyses revealed in PC samples small volume fraction of nanoparticles with a size between 10–100 nm. EELS and EDX analyses have shown that they are rich in manganese. A small number of 10–30 nm in diameter oxides, in particular at the triple points/grain boundaries, have also been observed. On the other hand high Resolution STEM imaging has shown no amorphous layers along the grain boundaries, characteristic for oxides [18]. Also EELS analyses confirmed that there is no evidence of oxygen segregation to grain boundaries – see Fig. 3.
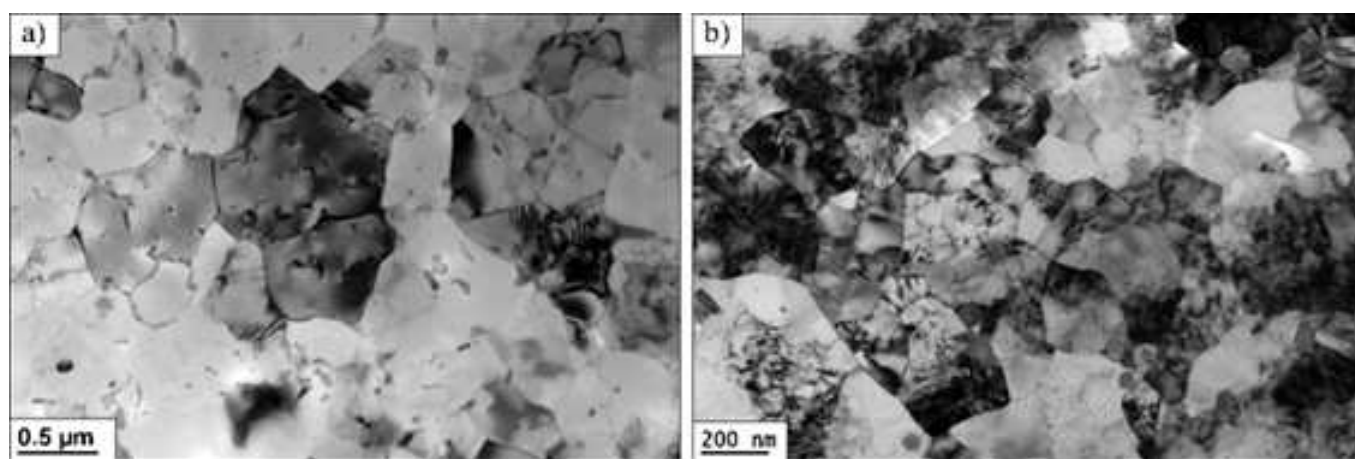

Fig. 1. TEM images of a) AA-5083 after plastic consolidation of powders, b) AA-5483 after hydrostatic extrusion
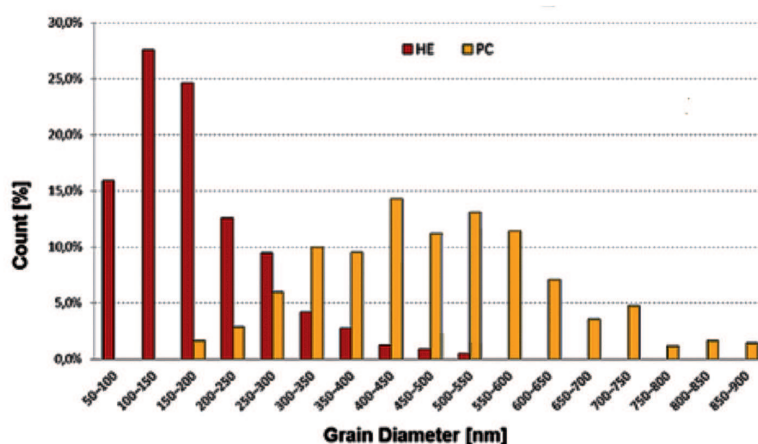

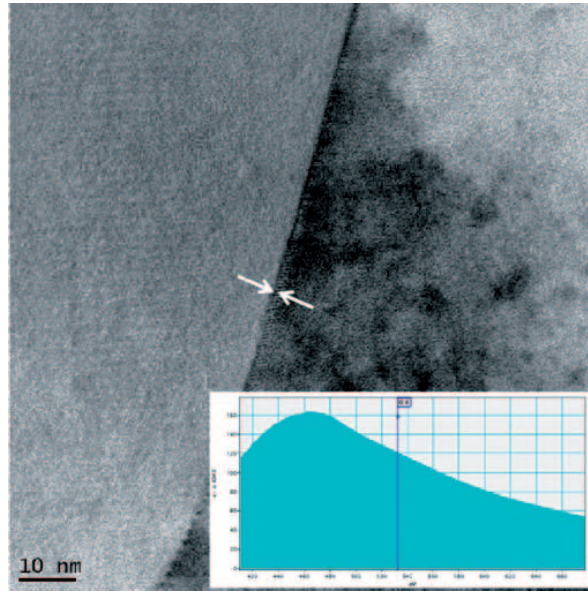Fig. 2. Grain size distribution in Pc and HE samples

Fig. 3. High resolution image of grain boundary together with EELS spectra taken from the grain boundary

The way of processing of the samples has also a significant impact on the distribution of grain boundary misorientation angles. Analysis of 100 grain boundaries for each material revealed in PC samples a large density of high angle grain boundaries (over 90% of the population analysed). In HE samples the density of high angle boundaries is much lower and below 45%. The distribution in this case is much wider with a significant fraction of low and medium grain boundaries – 12% and 45% respectively.

3.2. Mechanical properties

The properties determined in tensile tests are summarised in Table 2. It should be noted that both samples exhibit excellent strength exceeding 450 MPa, combined with a ductility which is exceptionally good for SPD processed billets, with elongation to failure above 10%. It should also be noted that in agreement with the known effect of grain size reduction and dislocation strengthening, HE samples feature higher strength while PC samples higher elongation.

TABLE 2

Tensile mechanical properties of PC and HE samples

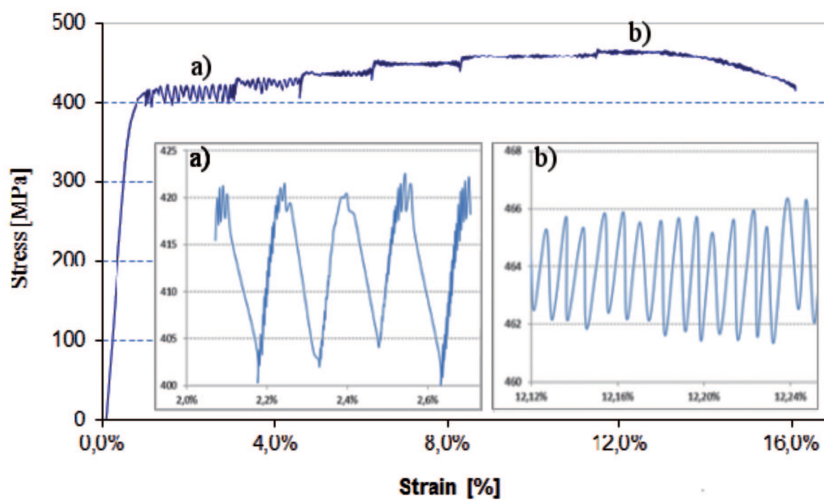| Sample	Ultimate Tensile Strength [MPa]	Yield Strength [MPa]	ε [%]	Strain-hardening exponent – n
5083 (PC)	465	380	15,5	0,122
5483 (HE)	545	490	12,1	0,115

Fig. 4. Stress-strain curve for tensile testing of Al-5083 after PC with expanded parts of this curve
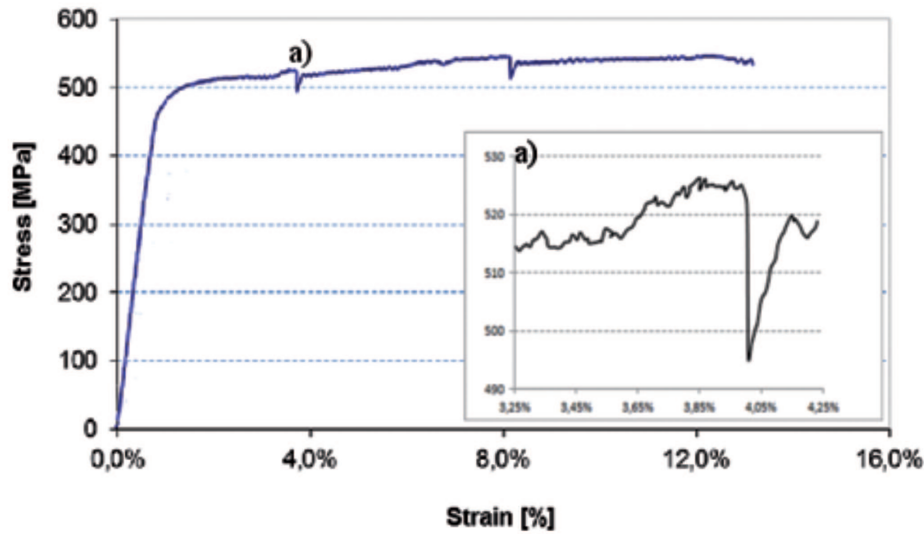
Fig. 5. Stress-strain curve for tensile testing of Al-5483 after HE with expanded part of this curve

As presented in Fig. 4 and 5, the tensile curves of both materials exhibit serrations (Portevin – Le Chatelier effect). The PLC effect in Al-Mg alloys is well described in the literature [1,19.,20]. Their average amplitude and frequency have been determined in order to quantify the intensity of serrations. From these results one can see that PLC effect in HE samples is relatively weak with the stress amplitude $\Delta\sigma = 1$ MPa and strain frequency $\Delta\varepsilon = 0,05\%$ being very low.

The serrations in PC samples feature different time-characteristics for different stages of deformation during tensile tests. A more detailed analysis indicates that in each subsequent stage, the stress amplitude decreases (it change from $\Delta\sigma = 17$ MPa at the first stage to $\Delta\sigma = 3$ MPa at the final stage of deformation) but the frequency of serration increases (from $\Delta\varepsilon = 0,15\%$ at the first stage to $\Delta\varepsilon = 0,01\%$ at the end).

4. Discussions

The experimental results presented in this paper clearly prove that both processing paths of Al 5XXX alloys investigated here open a promising route for improving their mechanical properties. It should be noted, however, that the two processing paths used in the present study result in different mechanical properties with ultrafine grained Al-Mg alloys obtained by top-down HE processing exhibiting higher strength in comparison to the ones obtained by bottom-up PC route.

In order to explain the unique properties of the samples studied here and differences between them it should be noted that the primary alloying element in both is magnesium (5wt.%), which at such a content forms a solid solution. The resulting solid solution strengthening can be quantified using the following formula:

$$\Delta\sigma_{SS} = HC^{\alpha} \qquad (2)$$

in which C is concentration of solute atoms and H and α are constants [21]. For HE samples with no precipitates observed, one can assume that all alloying elements are in the solid solution which gives = 85 MPa. In the case of PC samples, $\Delta\sigma_{SS}$ was estimated at 90 MPa due to the higher content of other elements, which also contribute to solution strengthening.

In a further analysis of the strength of both types of materials it should be pointed out that the HE processed is free of second phase particles. On the other hand, for PC samples second phase particles feature relatively large interparticle distance and their contribution is estimated at 50 MPa [2].

In agreement with the concept of the present study, the major strengthening mechanism for both materials is expected to be the grain boundary strengthening. Its contribution to the yield strength can be estimated from the HP relationship which predicts a linear dependence of yield stress on the inverse square root of grain size:

$$\Delta\sigma_{GB} = k_y d^{-1/2} \qquad (3)$$

where k_y is constant. For PC samples this formula gives $\Delta\sigma_{GB} = 221$ MPa and for HE samples $\Delta\sigma_{GB} = 325$ MPa. Both values are much higher than the effect of the solid solution.

Finally, one should also consider strengthening from dislocations, as their densities are relatively large, in particular in HE sample. Based on the calculated dislocation

densities, the contribution of strengthening arising from dislocations is estimated using the following formula:

$$\Delta\sigma_d = kl^{1/2} \qquad (4)$$

where: k – coefficient, typically 0,044 MPa m$^{1/2}$, l – the average distance between dislocations. This formula yields the following estimates of the strain hardening: 150 for HE and 24 MPa PC samples.

Assuming the additive character of the stress required to initiate plastic flow in materials considered, the following equation can be used to analyse their strength:

$$\sigma_y = \Delta\sigma_{SS} + \Delta\sigma_d + \Delta\sigma_{GB} \qquad (5)$$

This equation gives 555 and 385 MPa for HE and PC sample, respectively, which very well agree with the strength measured in the tensile tests - 490 and 380 MPa respectively.

It should be noted that the ultrafine grained Al-Mg samples obtained using two different approaches exhibit also a very good ductility with elongation to failure of more than 10%. Such a good ductility can be explained in terms of strain hardening during tensile deformation. By plotting stress-strain curves in double log coordinates it can be shown that the hardening coefficient n equals to 0.12 for both HE and PC samples. At the same time TEM observations revealed a significant increase in the dislocation density in tensile tested samples, as illustrated in Fig. 6 and 7 for HE and PC samples, respectively. The density of dislocations increases nearly an order of magnitude, (8 times – from $5 \cdot 10^{15}$ to $4 \cdot 10^{16}$ m^{-2})
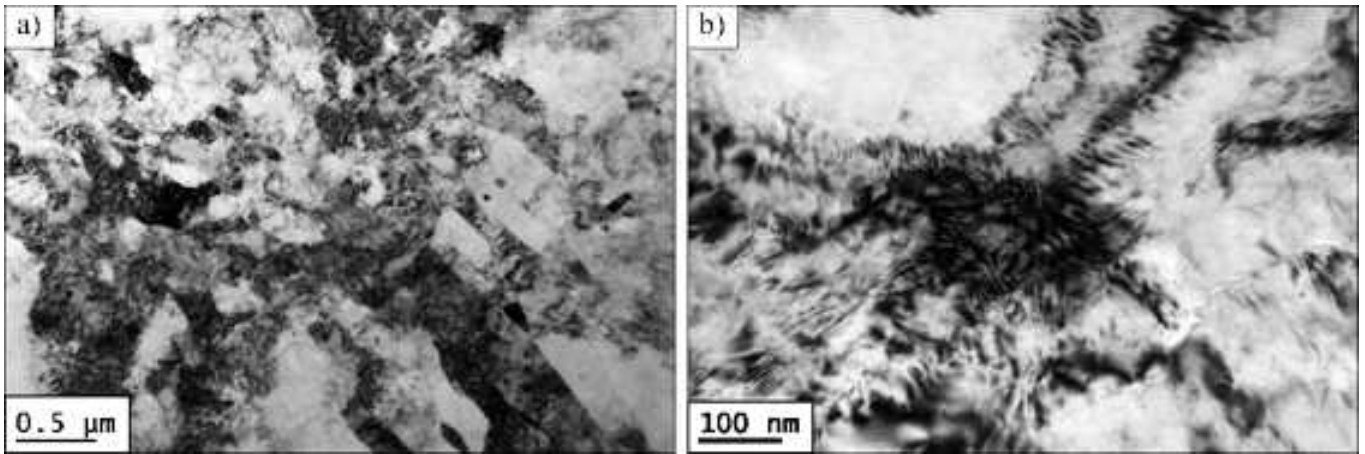

Fig. 6. TEM images of HE sample after tensile test, a) overall view of microstructure showing high density of dislocations in grains, b) image of grain boundaries with dislocation walls
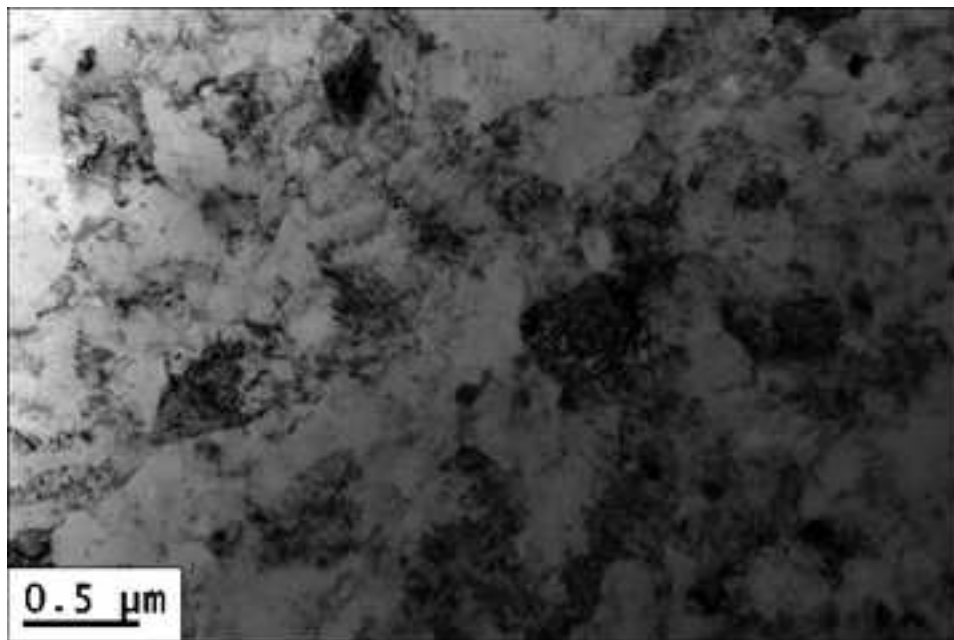

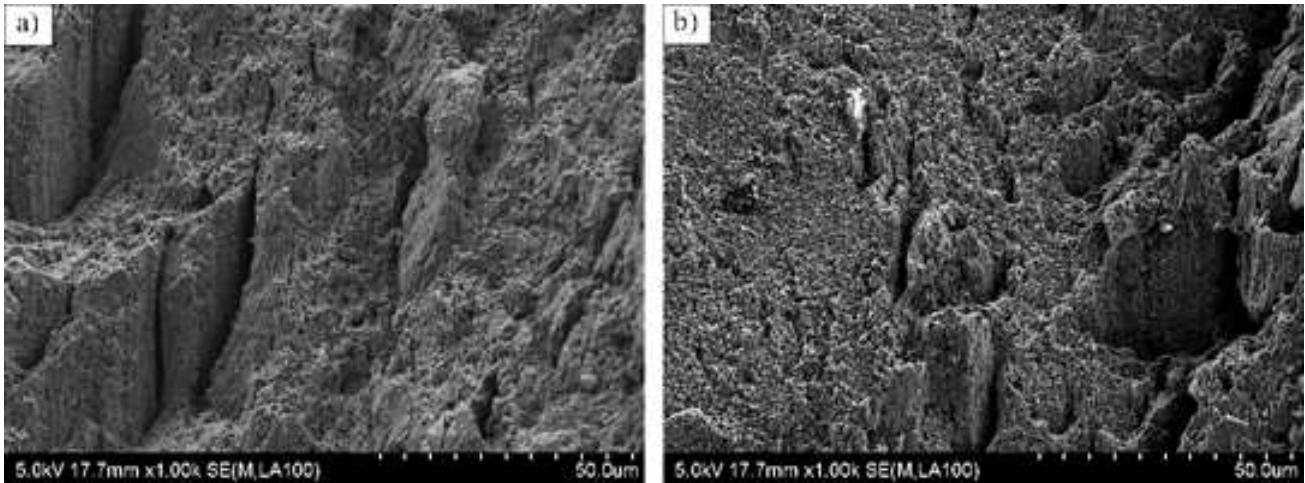Fig. 7. TEM image of PC sample after tensile tests

Fig. 8. Tensile fractures of a) PC and b) HE samples

for HE samples and two orders (from $1,2 \cdot 10^{13}$ m^{-2} to $2,5 \cdot 10^{15}$ m^{-2}) in the case of PC ones. This explains the better ductility of a PC sample. It should be noted that dislocations are distributed rather uniformly, tensile deformation neither changes the grain size nor results in shear banding. The capacity for plastic deformation is also confirmed by observations of fracture surfaces, illustrated in Fig. 8. Numerous small dimples typical for ductile fracture can be easily recognised. The fractures surfaces also exhibit smooth, flat areas separated by bright ridges.

As already stated, the characteristic features of mechanical behaviour of Al-Mg samples are serrations on tensile curves. In ultrafine grained samples these serrations differ significantly from the ones typical of the micrograined alloys in terms of the average strain frequency, $\Delta\varepsilon$, and stress amplitude $\Delta\sigma$ [1,22,23,24]. In particular, for HE samples, one can observe the combination of type A (jumps in stress) and B (weak serration occurring on the entire curve) serrations. Conventional Type A serrations (for micrograined alloy) can be characterised by a large amount of jumps in stress [23,24]. However, only few such jumps have been observed for ultrafine grained HE samples (2-3 in entire curve). These findings can be explained in terms of the interactions between dislocations, the density of which increases 8 times during tensile tests. The HE induced grain refinement also has an impact on their mobility, as the grain boundaries act as obstacles for dislocation movement.

In PC samples, serrated flow can be designated as Type D combined with Type B [23,24]. Type B serrations have a higher stress amplitude and frequency than in HE samples. It could be explained by referring to the same factors which influence mobility of dislocations. For micrograined materials, type D serration is attributed to the propagation of deformation bands [23,24]. This type of serration is usually observed at elevated temperatures. As no banding was observed in the present case, this finding needs further analysis and will be a subject of future work.

5. Conclusions

The following conclusions can be drawn from the results obtained in the present study:

Firstly, Al 5XXX alloys can be efficiently strengthened up to the flow stress exceeding 450 MPa by both Hydro Extrusion of solid billets and extrusion compaction of nano-powders. Despite the fact that both processing routes are essentially SPD based, samples obtained featured high elongation to fracture in the tensile tests, exceeding 10%.

Secondly, it should be noted that the excellent mechanical properties of alloys obtained can be explained in terms of the additive strengthening by solid solution, grain size reduction and strain hardening. Additive character of these three mechanisms has so far been postulated for micrograined alloys and its validation for sub-micron aluminium alloys opens new avenues for improving their mechanical properties.

Finally, it should be noted that PLC effects observed in ultrafine grained samples differ in type, frequency and amplitude from the ones described for micro-grained samples. This part of the study requires, however, more experimental evidence which is a subject of on-going research.

REFERENCES

[1] K.-D. Woo, S.-W. Kim, T.P. Lou, Mater. Sci. Eng. **A 334**, 157-261 (2002).

[2] E.L. Huskins, B. Cao, K.T. Ramesh, Mater. Sci. Eng. **A 527**, 1292-1298 (2010).

[3] M. Lewandowska, K.J. Kurzydłowski, Mater. Charact. **55**, 395-401 (2005).

[4] X. Yao, S. Zajac, B. Hutchinson, Scr. Mater. **41**, 3, 253-258 (1999).

[5] H. Hansen, Scr. Mater. **51**, 801-806 (2001).

[6] A. Azushima, R. Kopp, A. Korhonen, D.Y. Yang, F. Micari, G.D. Lahoti, P. Groche, J. Yanagimoto, N. Tsuji, A. Rosochowski, A. Yanagida, CRIP Annals – Manuf. Tech. **57**, 716-735 (2008).

[7] T. Qian, M. Marx, K. Schuler, M. Hockauf, H. Vehoff, Acta Mater. **58**, 2112-2123 (2010).

[8] R.K. Islamgaliev, N.F. Yunusova, I.N. Sabirov, A.V. Sergueeva, R.Z. Valiev, Mater. Sci. Eng. **A 319-321**, 877-881 (2001).

[9] R. Richert, Q. Liu, N. Hansen, Mater. Sci. Eng. **A 260**, 275-283 (1999).

[10] B. Cherukuri, T.S. Nedkova, R. Srinivasan, Mater. Sci. Eng. **A 410-411**, 394-397 (2005).

[11] N. Rangaraju, T. Raghuram, B.V. Krishna, K.P. Rao, P. Venugopal, Mater. Sci. Eng. **A 398**, 246-251 (2005).

[12] J.M. Gobien, R.O. Scattergood, F.E. Goodwin, C.C. Koch, Mater. Sci. Eng. **A 518**, 84-88 (2009).

[13] K.J. Kurzydlowski, Mater. Sci. Forum **503-504**, 341-348 (2006).

[14] M. Lewandowska, Solid State Phenomena **114**, 109-116 (2006).

[15] H. Dybiec, Arch. Metall. Mater. **52**, 161-170 (2007).

[16] Kyung-Tae Park, J.H. Park, Y.S. Lee, W.J. Nam, Mater. Sci. Eng. **A 408**, 102-109 (2005).

[17] D.M. Norfleet, D.M. Dimiduk, S.J. Polasik, M.D. Uchic, M.J. Mills, Acta. Mater. **56**, 2988-3001 (2008).

[18] L.P.H. Jeurgens, W.G. Sloof, F.D. Tichelaar, E.J. Mittemeijer, Thin Solid Films **418**, 89-101 (2002).

[19] D. Canadinc, H.J. Maier, P. Gabor, J. May, Mater. Sci. Eng. **A 496**, 114-120 (2008).

[20] K.-F. Zhang, H.-H. Yan, Trans. Nonferrous Met. Soc. China **19** 307-311 (2009).

[21] T. Suzuki, S. Takeuchi, H. Yoshinaga, Springer Series in Materials Science **12**, 32-44 (1990).

[22] J.M. Reed, M.E. Walter, Mater. Sci. Eng. **A 359**, 1-10 (2003).

[23] P. Podriguez, Bull. Mater. Sci. **6**, 4, 653-663 (1984).

[24] S.L. Mannan, Bull. Mater. Sci. **16**, 6, 561-582 (1993).